Thermal Conductivity and Diffusivity of High-Strength Polymer Fibers

1997 Jpn. J. Appl. Phys. 36 5633

(http://iopscience.iop.org/1347-4065/36/9R/5633)

Jpn. J. Appl. Phys. Vol. 36 (1997) pp. 5633–5637
Part 1, No. 9A, September 1997

Thermal Conductivity and Diffusivity of High-Strength Polymer Fibers

Hiroyuki FUJISHIRO[1], Manabu IKEBE[1], Toshihiro KASHIMA[2] and Atsuhiko YAMANAKA[2]
[1]*Faculty of Engineering, Iwate University, 4-3-5 Ueda, Morioka 020, Japan*
[2]*Research Institute, Toyobo Co., Ltd., 2-1-1 Katata, Ohtsu 520-02, Japan*

(Received March 12, 1997; accepted for publication June 2, 1997)

The thermal conductivity κ and diffusivity α of high-strength and high-modulus crystalline polymer fibers (polybenzobisoxazole (Zylon®) and polyethylene (Dyneema®)) and their fiber-reinforced plastics (FRPs) were measured in directions parallel and perpendicular to the molecular chain axis of the fibers. The main contribution to thermal conductivity was from phonon conduction along the molecular chains in both fibers and the phonon conduction was limited by boundary-like scattering over the temperature range of 10–260 K. From the analyses using a phenomenological model, the thermal conductivity anisotropy ratio ($\kappa_{/\!/}^{\rm fiber}/\kappa_{\perp}^{\rm fiber}$) of Zylon fiber was estimated to be 80 at 100 K, which was about two or three times larger than that of Dyneema fiber.

KEYWORDS: thermal conductivity, thermal diffusivity, polyethylene fiber, polybenzobisoxazole fiber, FRP, anisotropy ratio, phonon mean free path

1. Introduction

New high-performance fibers which have superior tensile strength and modulus to *p*-Aramid fibers have been developed recently and new applications using these fibers are being devised. These superior mechanical performances result from an improved crystallinity and higher orientation of molecular chains in the polymers, and both theoretical and experimental investigations have been performed.[1,2] Dyneema, which is a trade mark of TOYOBO in Japan, is one of these highly crystalline polyethylene fibers (crystallinity: ~80%) that has ultrahigh molecular weight, ultrahigh molecular chain orientation and excellent mechanical properties (tensile strength: 2.5 GPa and modulus: 88 GPa at 300 K). Poly *p*-phenylene-2,6-benzobisoxazole (Zylon; which is also a trade mark of TOYOBO in Japan) is a rigid-rod lyotropic liquid crystal fiber that has even better mechanical properties (tensile strength: 5.5 GPa and modulus: 280 GPa at 300 K). Figure 1 shows the molecular structures of Zylon and Dyneema. It would be very interesting to investigate how these mechanical properties are related to thermal properties such as thermal conductivity κ. Since the intrachain covalent bond is much stronger than the interchain van der Waals interaction in both systems, thermal conductivity parallel to the chains ($\kappa_{/\!/}$) is expected to be larger than that perpendicular to the chains ($\kappa_{\perp}$). It is well established that ultradrawing of high-density polyethylene fibers leads to a substantial increase in thermal conductivity ($\kappa_{/\!/}^{\rm fiber}$) and Young's modulus along the chain axis.[3,4] The thermal conductivity of these fibers depends on the crystallinity, the draw ratio and the production process.[5] From thermal measurements, we may obtain important revelations of the polymer structure which complement data from X-ray diffraction analysis and high-resolution electron microscopy. To date, conductivity measurements have been performed mainly for the $\kappa_{/\!/}$ component of the fibers. The thermal conductivity perpendicular to the chain axis ($\kappa_{\perp}^{\rm fiber}$) must also be characterized, although it is experimentally difficult to measure $\kappa_{\perp}^{\rm fiber}$.

We have developed a simultaneous measurement system for thermal conductivity κ and thermal diffusivity α using an identical experimental setup.[6,7] This system employs a Gifford-McMahon (GM) cycle helium refrigerator as a cryostat that enables measurements of κ and α between 10 and 260 K. Using this measurement system, we have investigated the thermal properties of several high-T_c superconductors (*e.g.*, $YBa_2Cu_3O_7$ and $(Bi, Pb)_2Sr_2Ca_2Cu_3O_X$) and analyzed the phonon conduction mechanisms.[7,8] We have also measured the thermal conductivity of composite materials such as $Ag + Bi_2Sr_2CaCu_2O_X$ and $Ag + YBa_2Cu_3O_7$ systems and distinguished contributions of each component to the conductivity based on a simple phenomenological model.[9,10]

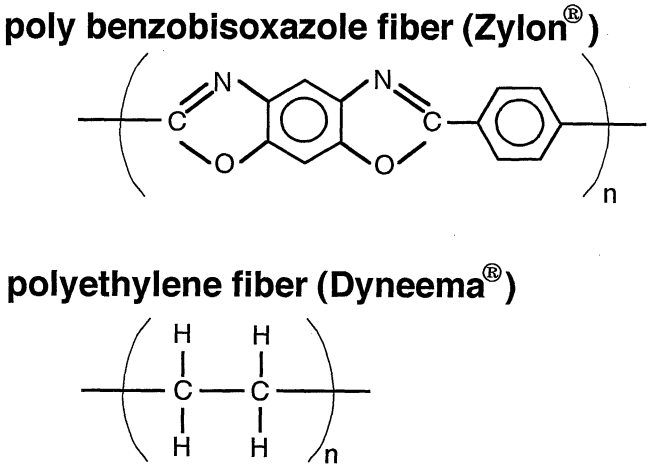

Fig. 1. Molecular structures of polybenzobisoxazole (Zylon®) and polyethylene (Dyneema®) fibers.

Fiber-reinforced plastics (FRPs) are examples of technological applications of these fibers. In cryogenic engineering, FRP is a popular construction material because it has high mechanical strength and low thermal conductivity suitable for use for an electrical and thermal insulating systems. Dyneema fiber (D-fiber) and its fiber-reinforced plastics (D-FRPs) also have excellent properties at low temperatures.[11,12] In this study, we determine the thermal conductivity κ and thermal diffusivity α of high-strength fibers (Z-fiber and D-fiber) and their FRPs (Z-FRP and D-FRP). κ and α of the FRPs

are measured in directions parallel and perpendicular to the embedded fibers and the anisotropic nature of thermal conduction is investigated. Based on a phenomenological heat conduction model, we discuss the anisotropy ratio of the fiber itself.

2. Experimental

2.1 Sample preparation

Fiber samples (Zylon and Dyneema:SK60) for measurement in the fiber direction ($\kappa_{/\!/}^{\rm fiber}, \alpha_{/\!/}^{\rm fiber}$) were prepared by bundling about 6000 monofilaments. The diameters of the monofilaments of Zylon and Dyneema, both of which were prepared by TOYOBO Co., Ltd., were about 10 μm and 12 μm, respectively. Both ends of the fiber bundle whose length was about 45 mm were fixed by an adhesive and intermediate positions where thermocouples were contacted were bound by fine (80 μm) Cu wire. Rectangular Z-FRP and D-FRP were fabricated with fiber volume fractions $V_{\rm f}$ ranging from 0.4 to 0.8. The samples used for measurement in the fiber direction ($\kappa_{/\!/}^{\rm FRP}, \alpha_{/\!/}^{\rm FRP}$) were about $2 \times 3 \times 25\,{\rm mm}^3$ with 25 mm length parallel to the fiber direction. The samples used for measurement in the perpendicular direction ($\kappa_{\perp}^{\rm FRP}, \alpha_{\perp}^{\rm FRP}$) were about $5 \times 4 \times 12\,{\rm mm}^3$ with 12 mm length perpendicular to the fiber direction. The density of each fiber was $1.57\,{\rm g/cm}^3$ for Zylon and $0.97\,{\rm g/cm}^3$ for Dyneema. The density D of these FRP samples was determined by $D = W/V$, where W is the sample weight and V, the sample volume. The filling factor to the ideal density was larger than 95% for $V_{\rm f} = 0.5 \sim 0.8$ and about 85% for $V_f = 0.4$ for respective FRPs.

2.2 Measurement

One end of the sample (a fiber bundle and FRP) was attached to the cold stage of a GM refrigerator by the method of mechanical pressing using indium metal. A small resistance heater (1 kΩ) was adhered to the other end of the sample using GE7031 varnish. Au(Fe:0.07 at%)-chromel thermocouples were used as thermometers which were adhered by silver paste. The sample space was evacuated to below 10^{-5} Torr by an oil diffusion pump. The automated measuring system of κ and α was operated in the temperature range from 10 to 260 K. κ was measured by a steady-state heat flow method using the relation $\kappa({\rm W/cm\,K}) = (\dot{Q}/\Delta T)(L/S)$, where $\dot{Q}$ is the heat flow per second, ΔT the temperature difference between thermometers, L the distance between the thermometers and S the cross section of the sample. Thermal diffusivity α was measured by an arbitrary heating method which is one of the non-steady-state heating methods. Time evolutions of temperature at two measurement points were recorded after applying heat pulse from the heater and the measured temperature change was compared with the calculated ones for various α values. The one-dimensional diffusion equation was numerically solved using the measured temperature change at the position nearest the heater as a boundary condition. Details of the determination of α were described elsewhere.[6,7]

3. Experimental Results

3.1 Z-fiber and Z-FRP

Figure 2 shows the temperature dependence of κ in the fiber direction of Z-fiber ($\kappa_{/\!/}^{\rm fiber}$) and several Z-FRPs ($\kappa_{/\!/}^{\rm FRP}$) with various V_f values. For Z-FRP with $V_f = 0.6$, κ was also measured in the direction perpendicular ($\kappa_{\perp}^{\rm FRP}$) to the fiber axis. The measured $\kappa(T)$ of epoxy resin ($\kappa_{\rm E}$) used for FRP is also shown in the figure. In the measurement conducted in the fiber direction, the magnitude of thermal conductivity of Z-FRP significantly depended on V_f. For the FRP samples with the same V_f of 0.6, the thermal conductivity parallel to the fiber direction ($\kappa_{/\!/}^{\rm FRP}$) was about one order of magnitude larger than that perpendicular to the fiber direction ($\kappa_{\perp}^{\rm FRP}$). κ of the epoxy matrix was as small as 0.002 W/cm K at 100 K.

Figure 3 shows the thermal diffusivity α of Z-fiber ($\alpha_{/\!/}^{\rm fiber}$) and Z-FRPs ($V_{\rm f} = 0.6$) in the fiber direction ($\alpha_{/\!/}^{\rm FRP}$) and in the perpendicular direction ($\alpha_{\perp}^{\rm FRP}$). α of the epoxy matrix ($\alpha_{\rm E}$) is also shown in the figure. $\alpha_{/\!/}^{\rm fiber}$ showed very slight temperature dependence, whereas $\alpha_{\rm E}$ markedly increased with decreasing temperatures. The temperature dependence of $\alpha_{\perp}^{\rm FRP}$ was larger than that of $\alpha_{/\!/}^{\rm FRP}$ and increased by about one order of magnitude from 260 K down to 10 K. It was found that $\alpha_{/\!/}^{\rm FRP}$ was about one order of magnitude larger than $\alpha_{\perp}^{\rm FRP}$ and an anisotropy similar to κ was observed.

3.2 D-fiber and D-FRP

Figure 4 shows the temperature dependence of κ of D-fiber ($\kappa_{/\!/}^{\rm fiber}$) and D-FRP in parallel ($\kappa_{/\!/}^{\rm FRP}, V_{\rm f} = 0.6$) and in perpendicular ($\kappa_{\perp}^{\rm FRP}, V_{\rm f} = 0.6$) directions. $\kappa_{\rm E}$ is also shown in the figure. Similarly to Z-FRP, $\kappa_{/\!/}^{\rm FRP}$ was about one order of magnitude larger than $\kappa_{\perp}^{\rm FRP}$.

Figure 5 shows the thermal diffusivity $\alpha_{/\!/}^{\rm fiber}$ of D-fiber, as well as $\alpha_{/\!/}^{\rm FRP}$ and $\alpha_{\perp}^{\rm FRP}$ of D-FRPs ($V_{\rm f} = 0.6$). $\alpha_{\rm E}$ is

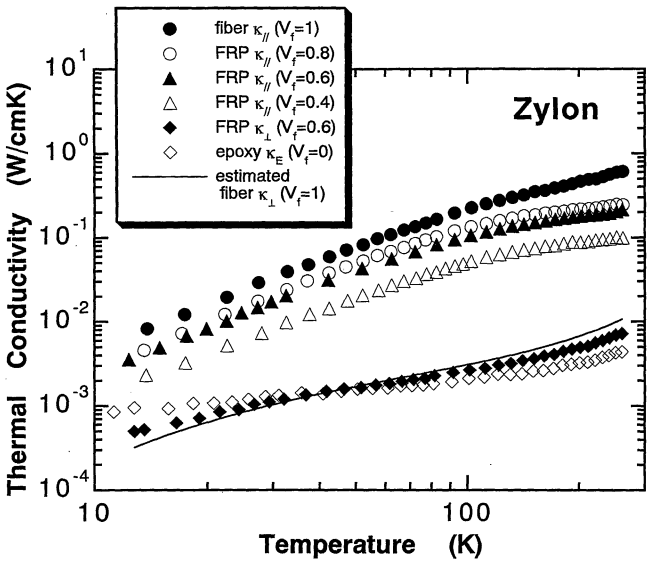

Fig. 2. Temperature dependence of thermal conductivity κ of Z-fiber ($\kappa_{/\!/}^{\rm fiber}$: $V_{\rm f} = 1$), several Z-FRPs ($\kappa_{/\!/}^{\rm FRP}$: $V_{\rm f} = 0.4$–0.8), Z-FRP ($\kappa_{\perp}^{\rm FRP}, V_{\rm f} = 0.6$) and epoxy resin ($\kappa_{\rm E}$: $V_{\rm f} = 0$). The estimated $\kappa_{\perp}^{\rm fibercal}$ for Zylon is also shown (see §4.2).

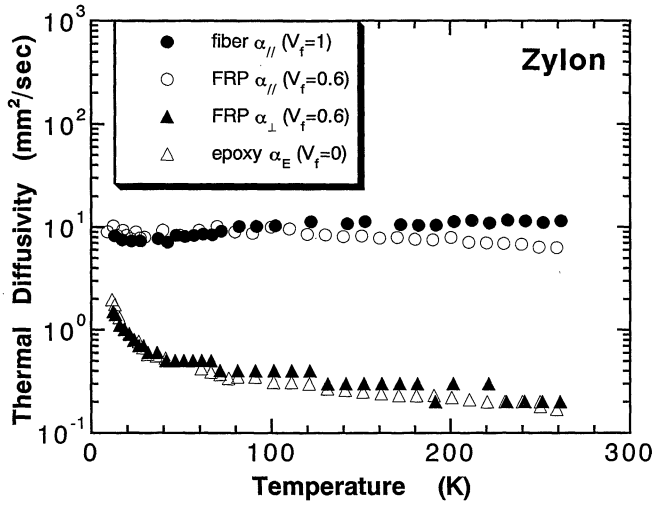

Fig. 3. The temperature dependence of thermal diffusivity α of Z-fiber ($\alpha_{//}^{\text{fiber}}$: $V_f = 1$), Z-FRPs ($\alpha_{//}^{\text{FRP}}$ and $\alpha_{\perp}^{\text{FRP}}$, $V_f = 0.6$) and epoxy resin (α_E: $V_f = 0$).

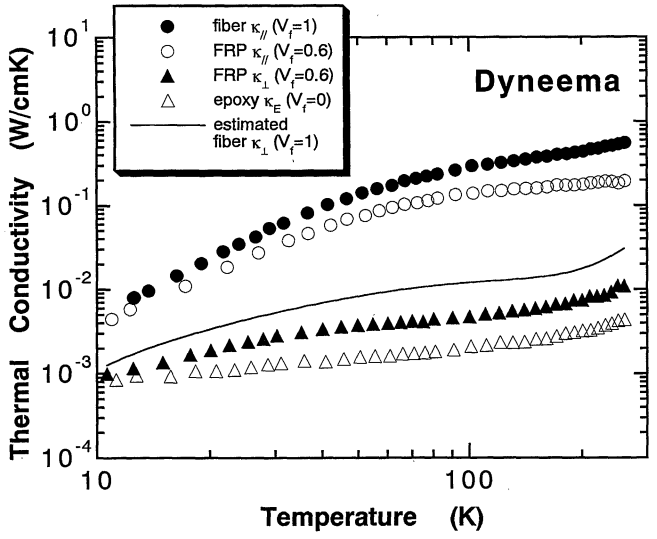

Fig. 4. Temperature dependence of thermal conductivity κ of D-fiber ($\kappa_{//}^{\text{fiber}}$: $V_f = 1$), D-FRPs ($k_{//}^{\text{FRP}}$ and $\kappa_{\perp}^{\text{FRP}}$, $V_f = 0.6$) and the epoxy resin (κ_E: $V_f = 0$). The estimated $\kappa_{\perp}^{\text{fibercal}}$ for Dyneema is also shown (see §4.2).

also shown in the same figure. It was found that $\alpha_{//}^{\text{FRP}}$ was about one order of magnitude larger than $\alpha_{\perp}^{\text{FRP}}$ and that anisotropy also existed. The temperature dependence and the absolute value of $\alpha_{//}^{\text{FRP}}$ are almost the same as those of Z-FRP in Fig. 3, but $\alpha_{\perp}^{\text{FRP}}$ of D-FRP is somewhat larger than that of Z-FRP. $\alpha_{//}^{\text{fiber}}$ of Dyneema also showed no marked temperature dependence.

4. Discussion

4.1 Model for analyses

Data from Figs. 2 to 5 offer valuable information regarding the application for a support material to cryogenic engineering systems.[11,12] From also the viewpoint of physics and chemistry, it would be interesting to investigate thermal anisotropy of the fibers themselves and the mechanisms of heat conduction. It is geometrically impossible to measure directly thermal conductivity perpendicular to the fiber direction ($\kappa_{\perp}^{\text{fiber}}$). Thus, we attempted to estimate $\kappa_{\perp}^{\text{fiber}}$ values from the measured data of FRPs using a model analysis. We have performed a model analysis of thermal conduction for composite materials.[9,10] In this paper we propose a revised model which is appropriate for the actual FRP structure. In FRPs, a number of monofilaments of Zylon or Dyneema are aligned and immersed in epoxy resin, each monofilament piercing the epoxy matrix from one end to the other end (see Fig. 6(a)). Figure 6(b) shows a model cube for the present analyses. In the cubic FRP sample with sides of length a, all of the monofilaments are concentrated into a rectangular bar that is embedded into the epoxy matrix. The cross section of the rectangular bar is $V_f a^2$. We assume that the thermal resistance of this model FRP cube approximates that of the real FRP sample. When heat flows in the fiber direction (along the y-axis), the heat flux should be parallel to the fiber and the epoxy, and thermal resistance $W_{//}^{\text{FRP}}$ is given by an equivalent circuit schematically shown in Fig. 6(c),

$$\frac{1}{W_{//}^{\text{FRP}}} = \frac{1}{W_{\text{E0}}} + \frac{1}{W_{//}^{\text{fiber}}} = a\kappa_{//}^{\text{FRP mes}}, \qquad (1)$$

where $W_{\text{E0}}\{= 1/[(1 - V_f)a\kappa_E]\}$ is the thermal resistance of epoxy resin, and $W_{//}^{\text{fiber}}[= 1/(V_f a\kappa_{//}^{\text{fiber}})]$ is that of fibers parallel to the fiber direction.

On the other hand, when heat flows perpendicular to the fiber direction (along the x-axis), thermal resistance $W_{\perp}^{\text{FRP}}$ is given by an equivalent circuit as shown in Fig. 6(d),

$$\frac{1}{W_{\perp}^{\text{FRP}}} = \frac{1}{W_{\text{E2}}} + \frac{1}{W_{\text{E1}} + W_{\perp}^{\text{fiber}} + W_c} = a\kappa_{\perp}^{\text{FRP mes}}, \qquad (2)$$

where $W_{\text{E1}}[= (1 - V_f)/(\sqrt{V_f}a\kappa_E)]$ and $W_{\text{E2}}\{= 1/[(1 - \sqrt{V_f})a\kappa_E]\}$ are the thermal resistance of epoxy resin in the sample and $W_{\perp}^{\text{fiber}}[= 1/(a\kappa_{\perp}^{\text{fiber}})]$ is that of fibers perpendicular to the fiber direction. W_c is the thermal contact resistance between the monofilaments and epoxy resin which impedes heat flow mainly in the perpendicular direction.

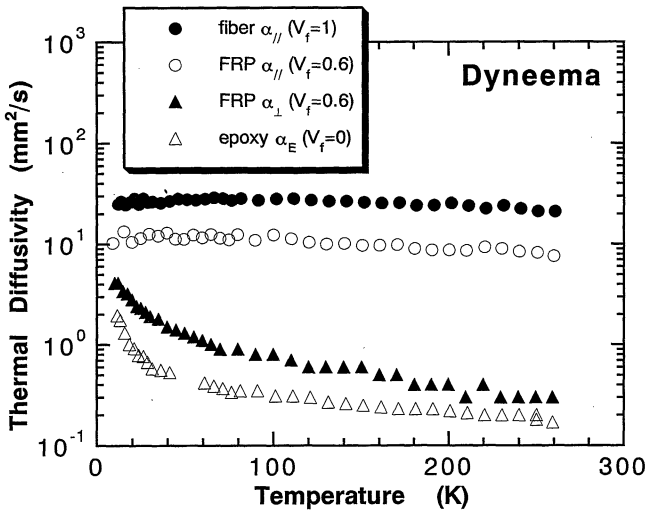

Fig. 5. Temperature dependence of thermal diffusivity α of D-fiber ($\alpha_{//}^{\text{fiber}}$: $V_f = 1$), D-FRPs ($\alpha_{//}^{\text{FRP}}$ and $\alpha_{\perp}^{\text{FRP}}$, $V_f = 0.6$) and epoxy resin (α_E: $V_f = 0$).

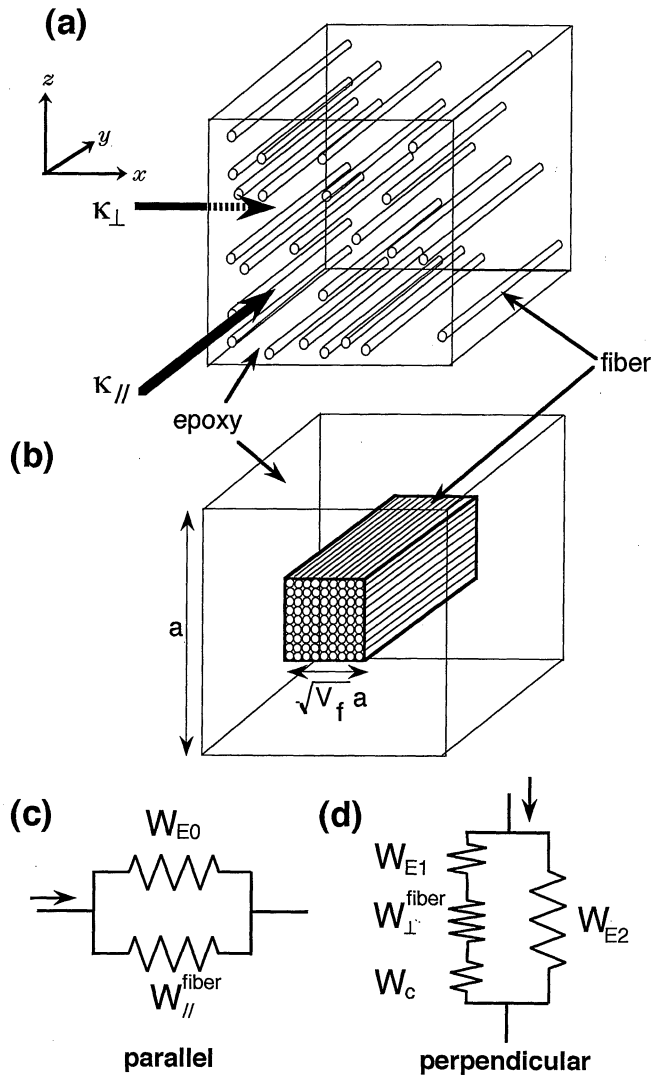

Fig. 6. The schematic diagram of the present model. (a) a real FRP in which the many monofilaments are aligned and immersed in epoxy resin: (b) a model cube of FRP for calculating κ in which all of the monofilaments are concentrated into a rectangular bar that is embedded into the epoxy matrix: (c) an equivalent circuit for calculating thermal resistance $W_{/\!/}^{\mathrm{FRP}}$ when heat flows parallel to the fiber direction (along the y-axis): (d) an equivalent circuit for calculating thermal resistance $W_{\perp}^{\mathrm{FRP}}$ when heat flows perpendicular to the fiber direction (along the x-axis).

4.2 Results of model calculation

Figure 7 shows the estimated thermal conductivity $\kappa_{/\!/}^{\mathrm{fibercal}}$ of Z-fiber in the Z-FRP at 20 K and 100 K, which was calculated using measured $\kappa_{/\!/}^{\mathrm{FRP\,mes}}$ data and eq. (1). The measured $\kappa_{/\!/}^{\mathrm{FRP\,mes}}$ data are also shown. The estimated $\kappa_{/\!/}^{\mathrm{fibercal}}$ for each V_f is almost equal to the measured $\kappa_{/\!/}^{\mathrm{fiber}}(V_f = 1)$ irrespective of V_f values, supporting the validity of the model analysis. Heat flow in the fiber direction can therefore be represented using the model shown in Fig. 6(c).

When we solve eq. (2) for $\kappa_{\perp}^{\mathrm{fiber}}$, we obtain the following equation;

$$\kappa_{\perp}^{\mathrm{fibercal}} = \frac{\sqrt{V_f}\kappa_{\mathrm{E}}\{(1-\sqrt{V_{\mathrm{f}}})\kappa_{\mathrm{E}} - \kappa_{\perp}^{\mathrm{FRP\,mes}}\}}{(1-\sqrt{V_f})\kappa_{\perp}^{\mathrm{FRP\,mes}} - \{(1-\sqrt{V_{\mathrm{f}}})^2 + \sqrt{V_f}\}\kappa_{\mathrm{E}}}, \tag{3}$$

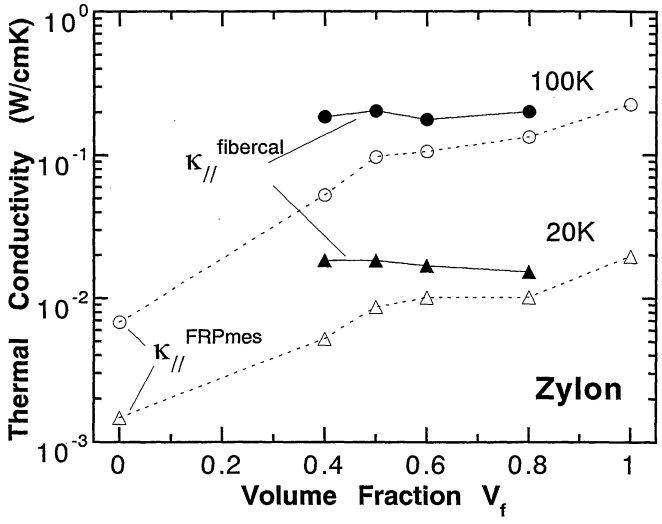

Fig. 7. Closed circles and triangles represent the calculated thermal conductivity of Zylon along the fiber direction at 20 K and 100 K. Open circles and triangles represent the measured thermal conductivity of Z-FRP parallel to the embedded fiber axis. Note that ○ and △ at $V_{\mathrm{f}} = 0$ and 1 correspond to the thermal conductivity of epoxy matrix and Zylon.

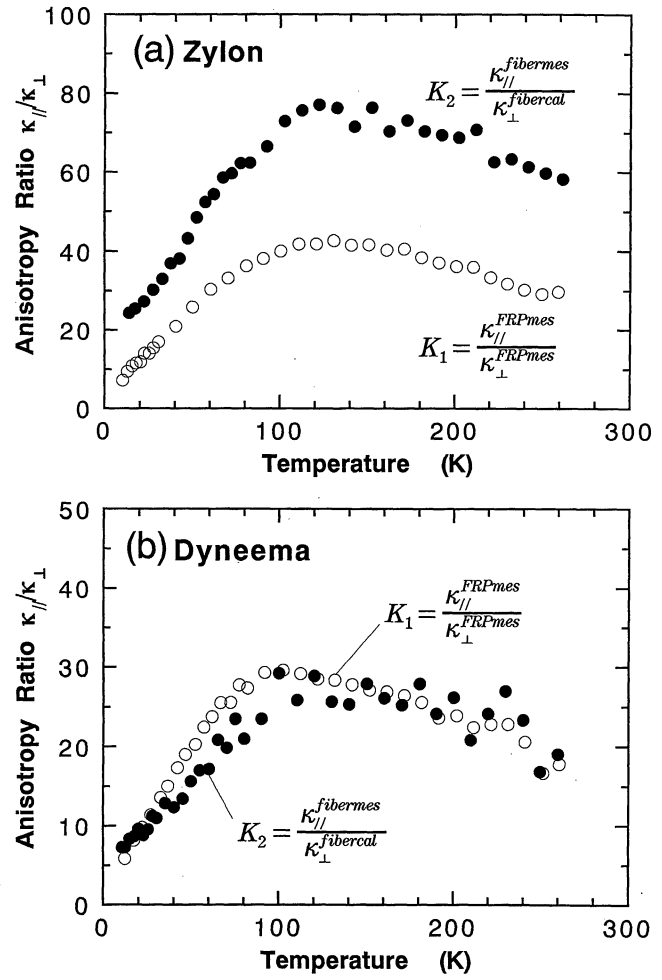

Fig. 8. Anisotropy ratio $\kappa_{/\!/}/\kappa_{\perp}$ for (a) Zylon and Zylon-FRP, and (b) Dyneema and Dyneema-FRP. $K_1 = (\kappa_{/\!/}^{\mathrm{FRP\,mes}})/(\kappa_{\perp}^{\mathrm{FRP\,mes}})$ represents the ratio of the κ measured in the parallel direction to that measured in the perpendicular direction for FRP ($V_{\mathrm{f}} = 0.6$) samples and $K_2 = (\kappa_{/\!/}^{\mathrm{fibermes}})/(\kappa_{\perp}^{\mathrm{fibercal}})$ shows the ratio of the measured κ of fiber ($\kappa_{/\!/}^{\mathrm{fibermes}}$) to the estimated κ ($\kappa_{\perp}^{\mathrm{fibercal}}$) using eq. (3).

where the contact resistance W_c is ignored. The estimated $\kappa_{\perp}^{\text{fibercal}}$ using measured $\kappa_{\perp}^{\text{FRP mes}}$ ($V_f = 0.6$) data is shown in Fig. 2 for Zylon and Fig. 4 for Dyneema. $\kappa_{\perp}^{\text{fibercal}}$ for Zylon is larger than the measured $\kappa_{\perp}^{\text{FRP}}$ from 50 K to 260 K and smaller below 50 K. For Dyneema, $\kappa_{\perp}^{\text{fibercal}}$ is larger than the measured $\kappa_{\perp}^{\text{FRP}}$ in the entire temperature range. Figure 8 shows the anisotropy ratio $\kappa_{/\!/}/\kappa_{\perp}$ of the thermal conductivity for (a) Zylon and Z-ERP, and (b) Dyneema and D-FRP. $K_1 = (\kappa_{/\!/}^{\text{FRP mes}})/(\kappa_{\perp}^{\text{FRP mes}})$ represents the measured ratio of thermal conductivities of FRP samples with $V_f = 0.6$. $K_2 = (\kappa_{/\!/}^{\text{fibermes}})/(\kappa_{\perp}^{\text{fibercal}})$ represents the ratio of measured κ in the fiber direction ($\kappa_{/\!/}^{\text{fibermes}}$) to κ in the perpendicular direction ($\kappa_{\perp}^{\text{fibercal}}$) estimated using eq. (3). For Zylon, K_1 is about 40 and K_2 is about 80, both of which show a maximum around 130 K. K_1 and K_2 for Dyneema are about 30 and show a maximum around 100 K. K_1 and K_2 for Dyneema are almost the same because the estimated $\kappa_{\perp}^{\text{fibercal}}$ value and the κ_E value of the epoxy matrix are similar. The difference in anisotropy ratio for each system may result from the difference in the molecular structure and/or the thermal contact resistance between the fibers and epoxy resin. The anisotropy ratio $\kappa_{/\!/}/\kappa_{\perp}$ of thermal conductivity for polyethylene fibers was reported to be about 5 by Burgess and Greig[5] and about 3000 by Choy *et al.*[13] and the values were very scattered. In this study, we estimated the perpendicular thermal conductivity $\kappa_{\perp}^{\text{fibercal}}$ under the assumption that the thermal contact resistance W_c was zero. If non-zero values of W_c are confirmed experimentally by measurement of, for example, the S_f (=total surface of embedded fibers) dependence or the diameter dependence of $\kappa_{\perp}^{\text{FRP}}$, estimated intrinsic $\kappa_{\perp}^{\text{fibercal}}$ values will become larger, resulting in a smaller value of real K_2. Thus the present K_2 value will correspond to the maximum of the anisotropy ratio of the fibers. Because the contact resistance is known to become very large in low temperature region,[3,14] the effect of W_c will become more serious at low temperatures[3,14] and K_2 will become larger at low temperatures. In Fig. 8, however, K_2 takes a maximum at relatively high temperatures ($T_{\max} \geq 100$ K) and decreases with decreasing temperature. Thus W_c, if it exists, does not come from usual contact-type resistance. It seems that W_c does not play a major role in limiting $\kappa_{\perp}$ in the present FRP samples.

4.3 Thermal diffusivity and mean free path of phonons

Because Zylon and Dyneema are insulators, thermal conduction is due to only phonons. Then thermal diffusivity α is given by

$$\alpha = \frac{1}{3} v_{s/\!/} l_{/\!/}, \tag{4}$$

where $v_{s/\!/}$ is the sound velocity and $l_{/\!/}$ is the phonon mean free path parallel to the fiber axis. As can be seen in Figs. 3 and 5, α of Zylon and Dyneema fibers is nearly independent of temperature T. This result is in marked contrast with that obtained for ordinary solids in which phonons are scattered by various imperfections such as point defects and stacking faults. In case of phonon scattering by lattice defects, the mean free path always increases with decreasing temperature[15] and, accordingly, α increases with decreasing temperatures. The observed almost constant α of the fibers means a constant $l_{/\!/}$ of the fibers and the constant $l_{/\!/}$ means that phonons are mainly scattered by domain wall-like barriers over the entire temperature range. Using Young's modulus E and density ρ, $v_{s/\!/}$ is estimated to be 1.34×10^6 cm/s for Zylon and 0.95×10^6 cm/s for Dyneema. From these $v_{s/\!/}$ values and the measured α values, $l_{/\!/}$ is estimated to be 25 Å for Zylon and 60 Å for Dyneema. It is inferred that a characteristic structure of size comparable with $l_{/\!/}$ may exist inside each fiber.

Acknowledgements

The authors wish to thank N. Nakasato of Iwate University for his assistance in the calculations of thermal diffusivity. This work was performed at the Center for Cooperative Research and Development, Iwate University.

1) B. Dessain, O. Moulaert, R. Keunings and A. R. Bunsell: J. Mater. Sci. **27** (1992) 4515.
2) T. Okada, S. Nishijima, K. Takahata and J. Yamamoto: Cryogenics **31** (1991) 307.
3) C. L. Choy and K. Young: Polym. **18** (1977) 769.
4) C. L. Choy and W. P. Leung: J. Polym. Sci. **21** (1983) 1243.
5) S. Burgess and D. Greig: J. Phys C: Solid State Phys. **8** (1975) 1637.
6) H. Fujishiro, T. Naito, M. Ikebe and K. Noto: Cryo. Eng. **28** (1993) 533 [in Japanese].
7) M. Ikebe, H. Fujishiro, T. Naito and K. Noto: J. Phys. Soc. Jpn. **63** (1994) 3107.
8) H. Fujishiro, M. Ikebe, T. Naito, K. Noto, S. Kohayashi and S. Yoshizawa: Jpn. J. Appl. Phys. **33** (1994) 4971.
9) M. Ikebe, H. Fujishiro, M. Matsukawa, F. Tatezaki, H. Ogasawara, K. Noto, K. Michishita and Y. Kubo: Jpn. J. Appl. Phys. **33** (1994) 2004.
10) H. Fujishiro, K. Kusaka, M. Ikebe, H, Ogasawara and K. Noto: Cryogenics **34** (1994) ICEC Suppl. p. 231.
11) T. Kashima, A. Yamanaka, E. S. Yoneda, S. Nishijima and T. Okada: Adv. Cryo. Eng. **41** (1996) 441.
12) T. Kashima, A. Yamanaka, S. Nishijima and T. Okada: Adv. Cryo. Eng. **42** (1997) 147.
13) C. L. Choy, S. P. Wong and K. Young: J. Polym. Sci.: Polym. Phys. Ed. **23** (1985) 1495.
14) E. T. Swartz and R. O. Pohl: Rev. Mod. Phys. **61** (1989) 605.
15) R. Berman: *Thermal Conduction in Solids* (Clarendon Press, Oxford, 1975).